

Article

Discrete Dynamic Model of a Disease-Causing Organism Caused by 2D-Quantum Tsallis Entropy

Nadia M. G. Al-Saidi ¹, Husam Yahya ² and Suzan J. Obaiys ^{3,*}¹ Department of Applied Sciences, University of Technology, Baghdad 10066, Iraq² Computer Engineering Techniques, Faculty of Information Technology, Imam Ja'afar Al-Sadiq University, Baghdad 10064, Iraq³ Department of Computer Systems and Technology, Faculty of Computer Science and Information Technology, University Malaya, Kuala Lumpur 50603, Malaysia

* Correspondence: suzan@um.edu.my

Abstract: Many aspects of the asymmetric organ system are controlled by the symmetry model (R&L) of the disease-causing organism pathway, but sensitive matters like somites and limb buds need to be shielded from its influence. Because symmetric and asymmetric structures develop from similar or nearby matters and utilize many of the same signaling pathways, attaining symmetry is made more difficult. On this note, we aim to generalize some important measurements in view of the 2D-quantum calculus (q -calculus, q -analogues or q -disease), including the dimensional of fractals and Tsallis entropy (2D-quantum Tsallis entropy (2D-QTE)). The process is based on producing a generalization of the maximum value of the Tsallis entropy in view of the quantum calculus. Then by considering the maximum 2D-QTE, we design a discrete system. As an application, by using the 2D-QTE, we depict a discrete dynamic system that is afflicted with a disease-causing organism (DCO). We look at the system's positive and maximum solutions. Studies are done on equilibrium and stability. We will also develop a novel design for the fundamental reproductive ratio based on the 2D-QTE.



Citation: Al-Saidi, N.M.G.; Yahya, H.; Obaiys, S.J. Discrete Dynamic Model of a Disease-Causing Organism Caused by 2D-quantum Tsallis Entropy. *Symmetry* **2022**, *14*, 1677. <https://doi.org/10.3390/sym14081677>

Academic Editor: Hüseyin Budak

Received: 5 July 2022

Accepted: 8 August 2022

Published: 12 August 2022

Publisher's Note: MDPI stays neutral with regard to jurisdictional claims in published maps and institutional affiliations.



Copyright: © 2022 by the authors. Licensee MDPI, Basel, Switzerland. This article is an open access article distributed under the terms and conditions of the Creative Commons Attribution (CC BY) license (<https://creativecommons.org/licenses/by/4.0/>).

Keywords: quantum calculus; fractal; Tsallis entropy; discrete dynamic system; equilibrium point

1. Introduction

The history of quantum calculus, often referred to as the q -derivative, Jackson derivative, or q -disease, and dating back three centuries to the works of Bernoulli and Euler, is one of the most challenging math topics to grasp [1]. The q -derivative actions are now developing swiftly due to their versatility in fields like mathematics, mechanics, and physics. Quantum mechanics, analytic number theory, special functions theory of finite differences, Bernoulli and Euler polynomials, combinatorial, entropy definition, information theory, the theory of computer science, computational studies, image processing, chemical processing, data sciences, umbral derivative, Sobolev fractional norms, operator principle, and more recently, the idea of geometric functions theory, all benefit from the wide variety of applications of q -derivative (see [2–5]).

For a very long time, discrete dynamic systems of DCO were the subject of intense discussion because they were successful at describing the process of disease dissemination (see [6]). The classic DCO was provided in the prior twenty centuries [7]. Following that, a huge number of publications on DCO [8–10] were established. Overall, DCOs are thought to be homogeneously mixed, which means that the same information is spread to those who are susceptible. However, there are several systems of populations in humanoid society, and linking between individuals is not always the same [11]. The fundamental reproductive ratio [12] is used to study the stability and convergence of the structures. Depending on the system and circumstances of the solution, this ratio is expressed in several formulas. We propose novel formalization of this ratio based on the entropy idea in our argument.

Pastor–Satorras and Vespignani [13] developed different studies of epidemics and vaccination in scale-free networks. Colizza et al. [14] proposed a dynamic system of response–dispersion procedures and met inhabitants’ simulations in heterogeneous networks. Kanget et al. [15] investigated the diffusion dynamics of a model with a delay on scale-free networks. Łukasz and Toyozumi [16] analyzed the infection curvatures on human networks, which indicated that they are linear only in the vicinity of the critical point. Bae and Lee investigated the DCO epidemics on self-motivated network models with impermanent connection deactivation control structures [17].

With regard to the 2D-quantum calculus, which includes the dimension of fractals and 2D-QTE, we intend to specify certain relevant measures in this annotation. As an example, we illustrate a discrete dynamic system with a DCO utilizing the 2D-QTE. We consider the system’s best and most ideal options. Stability and equilibrium are studied. We will correspondingly enhance a novel 2D-QTE-based model for the basic reproductive ratio.

2. Methodology

2.1. Quantum Calculus

We start with the following definition. Jackson was the first to use the q -derivative [1] as follows: for $q \in (0, 1)$, a real interval, where $0 \in I$, and a function $\varphi : I \rightarrow \mathbb{R}$, the quantum derivative is given by the difference formula

$$\Theta^q[\vartheta](\chi) = \frac{\vartheta(q\chi) - \vartheta(\chi)}{\chi(q-1)}, \quad \chi \neq 0, \quad \Theta^q[\vartheta](0) = \vartheta'(0).$$

Meanwhile, the h -derivative is formulated by the structure [18]

$$\Sigma^h[\sigma](\chi) = \frac{\sigma(\chi+h) - \sigma(\chi)}{h}, \quad \chi \neq 0, h > 0.$$

In [19], Hahn proposed a difference operator as a method for building orthogonal polynomial families. Jackson’s q -difference operator and the forward difference operator are combined in Hahn’s quantum difference operator (in the limit)

$$\Delta^{q,\omega}[f](\chi) = \frac{f(q\chi + \omega) - f(\chi)}{\chi(q-1) + \omega}, \quad \chi \neq \omega_0 := \frac{\omega}{1-q}.$$

More generalizations of two dimensional quantum calculus are given by Chakrabarti and Jagannathan [20]

$$D^{q,\omega}[f](\chi) = \frac{f(q\chi) - f(\omega\chi)}{\chi(q-\omega)}$$

where

$$[n]_{q,\omega} = \frac{q^n - \omega^n}{q - \omega}, \quad (q \neq \omega).$$

Note that when $\omega = 1$, the quantum number reduces to the Jackson definition

$$[n]_q = \frac{q^n - 1}{q - 1}, \quad q \in (0, 1).$$

Based on the two-dimensional quantum structure, we shall generalize the definition of Tsallis’ entropy to obtain 2D-QTE and the fractal dimension formula.

2.2. Quantum Entropy

The Rudolf Clausius proposed entropy function is interpreted as statistical entropy by using probability theory in conventional statistical methods. The efforts of physicist Ludwig Boltzmann in the 19th century created the statistical entropy viewpoint. Tsallis extended this entropy to introduce the generalized fractional entropy, which is as follows [21]: let

$\{\rho_i\}$ be a discrete set of probabilities achieving the sum $\sum_i^n \rho_i = 1$, and τ any real number, and the Tsallis entropy can be realized by the structure

$$\begin{aligned} \mathbb{T}_\tau(\rho_i) &= \frac{1}{\tau-1} \left(1 - \sum_i^n \rho_i^\tau \right), \quad \tau \neq 1 \\ &= \left(\frac{1}{\tau(1-\frac{1}{\tau})} \left(1 - \sum_i^n \rho_i^\tau \right) \right) \\ &= \frac{1}{\tau} \left(\frac{1 - \sum_i^n \rho_i^\tau}{1 - \frac{1}{\tau}} \right). \end{aligned}$$

In view of [22], the maximum value determining when each micro-state is equiprobable $\rho_i = 1/\omega$; therefore

$$\mathbb{T}_\tau(\rho_i)^{\max} = \frac{1 - \omega^{1-\tau}}{\tau - 1}$$

Now the inequality $1/\tau \geq \omega$ and the solvability of the inequality $\omega^{1-\tau} - \omega^\tau \geq 0$ implies that

$$\mathbb{T}_\tau(\omega)^{\max} = \frac{1}{\tau} \left(\frac{1 - \omega^\tau}{1 - \omega} \right).$$

Consequently, by considering the quantum discussion, we receive the 2D-QTE

$$\begin{aligned} [\mathbb{T}_\tau]_{q,\omega} &= \frac{1}{\tau} \left(\frac{q^\tau - \omega^\tau}{q - \omega} \right) \\ &= \frac{1}{\tau} [\tau]_{q,\omega}, \quad q \neq \omega, \omega < q < 1. \end{aligned} \quad (1)$$

In applications, the value of ω is the total sum of the probability of the sample set such that $q > \omega$. Note that Equation (1) presents the maximum value of the Tsallis entropy in quantum calculus. The maximum values of Tsallis entropy is given in [22]. Moreover, Machado [23,24] proposed brand-new entropy formulations that were motivated by the behavior of fractional calculus [25]. Both common probability distributions and data series are used to explore the effects of the generalized fractional entropy. In addition, the researchers in [26] presented a generalized one-dimensional q -entropy utilizing the quantum deformed calculus.

2.3. 2D-Quantum Discrete System

In this part, we suggest the discrete system of the disease-causing organism (DCO) by using the 2D-quantum discrete operator. The transmission of the virus from the afflicted to the afflicted is governed by a number of factors. Additionally, illness dynamical systems can be studied under different rules for a single distinct individual, a small group of individuals, and a group of individuals as a whole. Depending on the complexity of the provided documents, many representations are chosen. Processors that produce the numbers and dispersion patterns of illnesses suggested systems in their modern incarnation (f.r. one can see [27–30]).

The DCO model is presented with N members and all of them are separated into n associations by their connections $i(i = 1, 2, \dots, n)$. Thus, it has $N = \sum_{i=1}^n N_i$, where N_i indicates the accumulated number of the members with sing i . It is assumed that every member has two sings, the infected (F) and the susceptible (P). The infected model may

enhance a vulnerable member with retrieval ratio ρ , and the susceptible member is infected with conveyance ratio ρ . Thus, we arrive at the equality

$$N_i(\chi) = P_i(\chi) + F_i(\chi)$$

and the discrete system

$$\begin{aligned} P_i(q\chi + \omega) &= P_i(\chi) \left(1 - \rho i \mathcal{U} [\mathbb{T}_\tau]_{q,\omega}(F_i(\chi))\right) + \rho \mathcal{U} F_i(\chi) \\ F_i(q\chi + \omega) &= F_i(\chi) \left(1 - \rho \mathcal{U}\right) + \rho \mathcal{U} P_i(\chi) [\mathbb{T}_\tau]_{q,\omega}(F_i(\chi)), \end{aligned} \quad (2)$$

$$\left(0 \leq P_i(0) \leq N_i, \quad 0 \leq F_i(0) \leq N_i\right)$$

where $[\mathbb{T}_\tau]_{q,\omega}(F_i(\chi))$ is the 2D-QTE created by the likelihood that any joint that already exists points to an infected node, where \mathcal{U} denotes the time-step measure. It is a value showing that the continuous DCO model can recognize the scheme (2) and that the equilibrium points of the structure (2) are identical to those of the continuous equivalent. Assume that

$$P(\chi) = \sum_{i=1}^n P_i(\chi), \quad \text{and} \quad F(\chi) = \sum_{i=1}^n F_i(\chi).$$

Then system (2) has the formula

$$\begin{aligned} P(q\chi + \omega) &= P(\chi) \left(1 - \rho \mathcal{U} [\mathbb{T}_\tau]_{q,\omega}(F(\chi))\right) + \rho \mathcal{U} F(\chi) \\ F(q\chi + \omega) &= F(\chi) \left(1 - \rho \mathcal{U}\right) + \rho \mathcal{U} P(\chi) [\mathbb{T}_\tau]_{q,\omega}(F(\chi)), \end{aligned} \quad (3)$$

$$\left(0 \leq P(0) \leq N, \quad 0 \leq F(0) \leq N, \quad \chi = 0, 1, 2, \dots\right).$$

To roughly equal the entropy model, we have

$$\begin{aligned} P(q\chi + \omega) &= P(\chi) - \rho i \mathcal{U} \Psi([\mathbb{T}_\tau]_{q,\omega}(F(\chi)), [\mathbb{T}_\tau]_{q,\omega}(P(\chi))) + \rho \mathcal{U} F(\chi) \\ F(q\chi + \omega) &= F(\chi) \left(1 - \rho \mathcal{U}\right) + \rho \mathcal{U} \Psi([\mathbb{T}_\tau]_{q,\omega}(F(\chi)), [\mathbb{T}_\tau]_{q,\omega}(P(\chi))), \end{aligned} \quad (4)$$

where the likelihood (probability) that every particular connect leads to an infected node is represented by the function F

$$[\mathbb{T}_\tau]_{q,\omega}(F(\chi)) = \frac{1}{\tau} \left(\frac{q^\tau - \omega_F^\tau}{q - \omega_F} \right), \quad \omega_F = 1/F;$$

similarly, for P , where

$$[\mathbb{T}_\tau]_{q,\omega}(P(\chi)) = \frac{1}{\tau} \left(\frac{q^\tau - \omega_P^\tau}{q - \omega_P} \right), \quad \omega_P = 1/P$$

and

$$\Psi([\mathbb{T}_\tau]_{q,\omega}(F(\chi)), [\mathbb{T}_\tau]_{q,\omega}(P(\chi))) = [\mathbb{T}_\tau]_{q,\omega}(F(\chi)) \times [\mathbb{T}_\tau]_{q,\omega}(P(\chi)).$$

Note that when $q, \omega \rightarrow 1^{-1}$, we obtain the model in [12], as follows:

$$\begin{aligned} P(\chi + 1) &= P(\chi) - \rho \mathcal{U} \Psi([\mathbb{T}_\tau]_{1,1}(F(\chi)), [\mathbb{T}_\tau]_{1,1}(P(\chi))) + \rho \mathcal{U} F(\chi) \\ F(\chi + 1) &= F(\chi) \left(1 - \rho \mathcal{U}\right) + \rho \mathcal{U} \Psi([\mathbb{T}_\tau]_{1,1}(F(\chi)), [\mathbb{T}_\tau]_{1,1}(P(\chi))), \end{aligned} \quad (5)$$

It is well known that the entropy-based structure of the function Ψ describes the interaction of susceptible and infected individuals in more generic terms. Entropy is an effective tool for analyzing probability distributions of a system's potential formal variables and, consequently, the information that system may hold. However, important details can be structured in time-based dynamics as well, a feature that is frequently overlooked. To find spatial structures and processes, the idea of planning entropy due to non-linear designs is used. Traditionally, linear spatial processes have been assumed, typically in terms of a linear autoregressive or heart-breaking average mode. Furthermore, potential spatial dynamics will demonstrate nonlinear types in a manner akin to time-based systems. Science is increasingly documenting the capabilities of nonlinear systems as the limitations of equilibrium representations in explaining real-world phenomena become more apparent. As a result, the benefit to scientific growth research is rising.

We continue to draw the conclusion that the Equation (4) has a solution.

Proposition 1. Consider the model (4). Then it admits a set of bounded nonnegative solutions whenever $\varrho\mathcal{U} \in (0, 1)$ for all $\tau > 1$.

Proof. System (4) satisfies the following inequality:

$$\begin{aligned} F(1) &= F(0) \left(1 - \varrho\mathcal{U}\right) + \rho i\mathcal{U} \Psi([\tau]_{q,\omega}(F(0)), [\tau]_{q,\omega}(P(0))) \\ &\leq N(1) + \rho i\mathcal{U} [\tau]_{q,\omega}(F) \times [\tau]_{q,\omega}(P) \\ &\leq N(1) + \frac{\rho i\mathcal{U} ([\tau]_{q,\omega})^2}{\tau^2}. \end{aligned}$$

By letting $\tau \rightarrow \infty$, we have $F(1)$ is positive and bounded by N . Hence, by induction, we confirm that $0 \leq F(\chi) \leq N$ for all $\chi = 0, 1, 2, \dots$. The above conclusion together with the fact $P(0) = 0$, implies that $P(\chi) \leq N$ for all $\chi = 0, 1, 2, \dots$. In addition, because $\varrho\mathcal{U} \in (0, 1)$ then $P(\chi) \rightarrow \varrho\mathcal{U}F(\chi) \geq 0$. We proved that model (4) admits a set of bounded nonnegative solutions. \square

3. Stability of DCO

In this part, we study the stability of DCO (2). Replacing $F_i(\chi) = N_i(\chi) - P_i(\chi)$ in the first equation of model (2), we get

$$\begin{aligned} P_i(q\chi + \omega) &= P_i(\chi) \left(1 - \rho i\mathcal{U} [\tau]_{q,\omega}(F_i(\chi))\right) + \varrho\mathcal{U} (N_i - P_i(\chi)) \\ F_i(q\chi + \omega) &= F_i(\chi) \left(1 - \varrho\mathcal{U}\right) + \rho\mathcal{U} P_i(t) [\tau]_{q,\omega}(F_i(\chi)), \end{aligned} \quad (6)$$

which is equivalent to the following system:

$$\begin{aligned} P_i(q\chi + \omega) &= P_i(\chi) \left(1 - \varrho\mathcal{U} - \rho i\mathcal{U} [\tau]_{q,\omega}(F_i(\chi))\right) + \varrho\mathcal{U} N_i(\chi) \\ F_i(q\chi + \omega) &= F_i(\chi) \left(1 - \varrho\mathcal{U}\right) + \rho\mathcal{U} P_i(t) [\tau]_{q,\omega}(F_i(t)). \end{aligned} \quad (7)$$

The disease-free equilibrium of DCO (7) can be calculated in view of the next formulation,

$$Y_0(P_1(0), \dots, P_n(0), F_1(0), \dots, F_n(0)) = (N_1, \dots, N_n, 0, \dots, 0).$$

Thus, the linearization matrix form of [31] on the model (7) at the point Y_0 is given, as follows:

$$\Pi = \begin{pmatrix} p + \ell & 0 \\ -p & \ell \end{pmatrix}_{2n \times 2n}, \quad (8)$$

where p indicates the vector of new infections and ℓ presents the vector of all other transitions containing disease-connected deaths. Note that they are nonnegative such that $p + \ell$ is irreducible and Π is the Jacobi matrix at Y_0 . Here, we suppose that this point is singular. We inform the following matrix:

$$p_{q,\omega} = \begin{pmatrix} \rho\mathcal{U}N_1[\top\tau]_{q,\omega} & \dots & \rho\mathcal{U}nN_1[\top\tau]_{q,\omega} \\ \rho\mathcal{U}N_n n[\top\tau]_{q,\omega} & \dots & \rho\mathcal{U}N_n n^2[\top\tau]_{q,\omega} \end{pmatrix}_{n \times n},$$

and

$$\ell = \begin{pmatrix} 1 - \rho\mathcal{U} & 0 & \dots & 0 \\ 0 & \dots & 0 & 1 - \rho\mathcal{U} \end{pmatrix}_{n \times n}.$$

Consequently, model (7) can be approximated by

$$\Delta(q\chi + \omega) \approx \Pi\Delta(\chi), \quad \Delta(\chi) = (P(\chi), F(\chi)), \quad \chi = 0, 1, 2, \dots$$

Because the proposed system is solely designed for diseased and susceptible individuals, we used the greatest value of 2D-QTE in it. The eliminated cases $\mathfrak{R}(\chi)$ were not included (death and recovery). The 2D-QTE can be used to define the following variable (see [32]):

$$\mathfrak{R}(\chi) = [\top\tau]_{q,\omega}(F(\chi)).$$

It should be noted that 2D-QTE is significantly correlated with the number of individuals N and groups n , ($1 \leq n \leq N$); therefore one should anticipate the DCO model conclusion to have non-linear incidence when $n = N$. Moreover, we can record that when $q \rightarrow 1$, we obtain the stability of the system [12]

$$p_{1,\omega} = \begin{pmatrix} \rho\mathcal{U}N_1[\top\tau]_{1,\omega} & \dots & \rho\mathcal{U}nN_1[\top\tau]_{1,\omega} \\ \rho\mathcal{U}N_n n[\top\tau]_{1,\omega} & \dots & \rho\mathcal{U}N_n n^2[\top\tau]_{1,\omega} \end{pmatrix}_{n \times n},$$

and

$$\ell = \begin{pmatrix} 1 - \rho\mathcal{U} & 0 & \dots & 0 \\ 0 & \dots & 0 & 1 - \rho\mathcal{U} \end{pmatrix}_{n \times n}.$$

The developers of [33] recently presented a q -statistical functional configuration that operates to acceptably characterize the information currently available for all areas. Computations of those peaks' dates and elevations in severely impacted nations are expected to occur unless well-planned interventions, vaccinations, or useful adjustments to the established epidemiological methodologies materialize.

3.1. 2D-Quantum Reproductive Ratio

The predicted ratio of cases openly created by one situation in a locality where all people are exposed to infection can be used to explain the elementary reproductive ratio ($\bar{\partial}_0$). Its name in mathematics is the spectral radius of the matrix $p(F - \ell) - 1$ (the major absolute amount of the eigenvalues).

There are numerous more descriptions and formulations that can accurately explain the circumstance. In order to achieve stability, this ratio is crucial. Much research has demonstrated that if $\bar{\partial}_0 > 1$, an unstable condition is indicated, and if $\bar{\partial}_0 < 1$, the situation is asymptotically stable, whereas if $\bar{\partial}_0 = 1$, indicates stability but nothing asymptotic [31].

Investigators recently proposed the situation casualty rate for the Corona virus (the aim is to reduce this ratio) [34]:

$$\mathfrak{R}(\chi) = \frac{D(\chi)}{F(\chi)}, \quad \chi = 0, 1, 2, \dots,$$

where D designs the total record of the death. For instance, if we have the following data, $D = 6$ and $F = 130$, then the ration is 1%. At the same time, if 130 of the 600 total susceptible individuals are noted, then

$$\mathfrak{R}_N(\chi) = \frac{D(\chi)}{F(\chi) + P(\chi)} = \frac{6}{600} = 1\%.$$

The goal is to place the person in an isolated position and continuously clean their surroundings in order to lower the rate \mathfrak{d}_0 or \mathfrak{R} . We recommend including the entropy assessment for this rate in our discussion. The authors of [35] used the probability of the survival function S to formulate \mathfrak{d}_0 as follows (for discrete data):

$$\mathfrak{d}_0 = \frac{F(\chi) \times S(\chi)}{N(\chi)}, \quad \chi = 0, 1, 2, \dots \quad N(\chi) = F(\chi) + S(\chi).$$

Consider the following data: $F = 130, D = 6$ and $N = 600$, and we have

$$\mathfrak{d}_0 = \frac{130 \times 0.783}{600} = 17\%.$$

The concept of the survival function’s probability is inappropriate for the corona virus. Consequently, based on our DCO model, we advise using the 2D-QTEQ $[\tau_\tau]_{q,\omega}$ as follows:

$$(\mathfrak{d}_0)_{q,\omega}^\tau = \frac{F(\chi) \times [\tau_\tau]_{q,\omega}(S(\chi))}{N(\chi)}, \quad \chi = 0, 1, 2, \dots \quad \tau \neq 1.$$

The stability of the system can be measured by the minimization of the ratio $(\mathfrak{d}_0)_{q,\omega}^\tau$. In view of our example, we check the ratio for the value 0.783, which represents the amount of ω . Consequently, we obtain the following table for the 2D-QTE and the ratio $(\mathfrak{d}_0)_{q,\omega}^\tau$ for different values of $\tau > 1$. Table 1 indicates some values of τ and the ratio $(\mathfrak{d}_0)_{q,0.783}^\tau$. Clearly increasing the value of τ implies decreasing the ratio $(\mathfrak{d}_0)_{q,0.783}^\tau$. That is, the suggested system is going well and healthy for analysis. As a conclusion, the system is stable whenever $\tau > 1$, whereas for $\tau < 1$, the system is unstable. The same result is shown in [12]. Figures refers the x-axis for q and the y-axis for \mathfrak{d}_0 . We get the following conclusion from the foregoing. Proposition 1 can be expanded to incorporate the stability as follows:

Proposition 2. Assume that the discreet model of DCO (4). If

$$q\mathcal{U} \in (0, 1), \quad \tau > 1 \tag{9}$$

then all solutions of (4) are bounded non-negative and stable achieving the following ratio

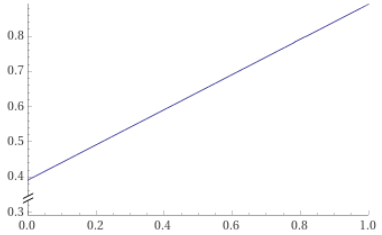
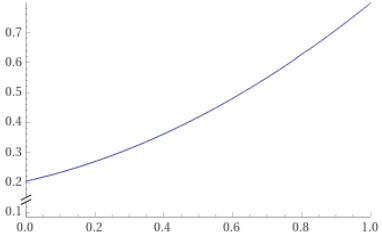
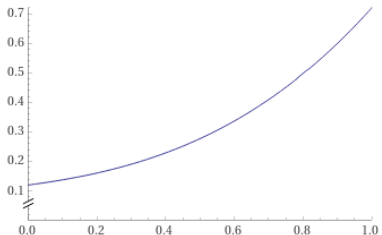
$$(\mathfrak{d}_0)_{q,\omega}^\tau = \frac{F(\chi) \times [\tau_\tau]_{q,\omega}(S(\chi))}{N(\chi)}, \quad \chi = 0, 1, 2, \dots \quad \tau \neq 1. \tag{10}$$

Proof. A direct application of Proposition 1. \square

Remark 1.

- The survival function, also known as the reliability function, is one of the methods used to formulate and display survival statistics. It provides the likelihood that a patient, plan, or other object of concern would survive longer than any given time. It gives the likelihood that a subject will live for more time than χ .
- A function like the exponential distribution may be able to accurately represent the survival times distribution. There are many distributions frequently used in survival analysis. These distributions are presented by parameters [36].
- Entropy is changed from a measure of information to a statistical tool by the entropy optimization principle, which also incorporates the 2D-QTE. It is safe to use this knowledge to define CFR because the greater maximum entropy belongs to fractional Tsallis entropy [37].

Table 1. The ratio $(\bar{\partial}_0)_{q,0.783}^\tau$.

τ	$\min \bar{\partial}_0$	Figure
2	0.4	
3	0.21	
4	0.12	

3.2. 2D-Fractal Dimensions

Finally, the formal for a real number considers the extended structure (multi-dimensions fractal) (MDF) $x \in \mathbb{R} \setminus \{1\}$ (see [38–40])

$$\Lambda_b(x) = \frac{1}{1-x} \lim_{b \rightarrow 0} \left(\frac{\log(Y(x,b))}{\log(1/b)} \right), \tag{11}$$

where

$$Y(x,b) = \sum_{k=1}^{N(b)} \rho_k^x.$$

Verify that every MDF in the aforementioned list satisfies the inequality below, which is a very helpful pattern for computing fractal dimensions in practice,

$$\Lambda_0 \geq \Lambda_1 \geq \dots \geq \Lambda_N.$$

According to information theory (also known as entropy theory) and using the item's values, the box-totaling dimension is determined as follows: [41,42]

$$\Lambda_b(x) = \frac{1}{1-x} \lim_{b \rightarrow 0} \left(\frac{\log(Y(x,b))}{\log(1/b)} \right) = \frac{1}{1-x} \lim_{b \rightarrow 0} \left(\frac{\log(T(x,b))}{\log(1/b)} \right), \quad (12)$$

where T stands for any entropy type.

The general dynamical, topological, and geometric characteristics of a given arrangement, as well as the higher order extensions $\Lambda_b(x)$, were each explained by using one of these MDFs. However, it is essential to comprehend how these assets change across different dimensions [43]. In this study, we suggest to improve (11) by utilizing the 2D-QTE, as follows:

$$\Lambda_{b,\omega}^{q,\tau}(x) = \frac{1}{1-x} \lim_{b \rightarrow 0} \left(\frac{\log([\top_\tau]_{q,\omega})}{\log(1/b)} \right), \quad (13)$$

where

$$[\top_\tau]_{q,\omega}(x,b) = \frac{1}{\tau} \left(\frac{q^\tau - \omega_x^\tau}{q - \omega_x} \right),$$

with $\omega_x = 1/\rho_{N(b)}^x$.

4. Conclusions

The study mentioned above demonstrated how numerous concepts, such as fractal dimensions and Tsallis-type entropy, have been generalized when utilizing quantum calculus in two dimensions. We used the suggested 2D-QTE in the DCO model's discrete dynamic system. Furthermore, we generalized the basic reproductive ratio. Under a straightforward set of circumstances, we investigated the system's existence and stability. Such a method will pave the way for numerous applications that use entropy as a measurement, including chaotic studies, image processing, and information theory.

The boundaries of many scientific disciplines, from computer science to mathematics and statistics to physics, chemistry, and engineering, have all paid close attention to quantum computation and quantum information. Data science integrates statistical techniques, computer algorithms, and information from domain sciences to draw knowledge and insights from large amounts of data and to address challenging real-world issues. Although it is well-known that quantum computation has the potential to revolutionize data science, much less has been said about the potential of data science to advance quantum computation. Yet because the stochasticity of quantum physics renders quantum computation random, data science can play an important role in the development of quantum computation and quantum information. This article gives an overview of quantum computation and promotes interplay between quantum science and data science. Overall, it advocates for the development of quantum data science for advancing quantum computation and quantum information.

Author Contributions: Conceptualization, N.M.G.A.-S. and S.J.O.; methodology, N.M.G.A.-S. and H.Y.; software, S.J.O. and N.M.G.A.-S.; formal analysis, N.M.G.A.-S., H.Y. and S.J.O.; investigation, N.M.G.A.-S. and S.J.O.; resources, S.J.O.; writing—original draft preparation, N.M.G.A.-S., H.Y. and S.J.O.; writing—review and editing, N.M.G.A.-S., H.Y. and S.J.O.; supervision, N.M.G.A.-S.; funding acquisition, S.J.O. All authors have read and agreed to the published version of the manuscript.

Institutional Review Board Statement: Not applicable.

Informed Consent Statement: Not applicable.

Data Availability Statement: Not applicable.

Conflicts of Interest: The authors declare no conflict of interest.

References

1. Jackson, F.H. XI. On q -functions and a certain difference operator. *Earth Environ. Sci. Trans. R. Soc. Edinb.* **1909**, *46*, 253–281. [[CrossRef](#)]
2. Ibrahim, R.W.; Ajaj, A.M.; Al-Saidi, N.M.G.; Balean, D. Similarity Analytic Solutions of a 3D-Fractal Nanofluid Uncoupled System Optimized by a Fractal Symmetric Tangent Function. *Comput. Model. Eng. Sci.* **2022**, *130*, 221–232. [[CrossRef](#)]
3. Al-Azawi; Al-Saidi, R.J.N.M.G.; Jalab, H.A.; Kahtan, H.; Ibrahim, R.W. Efficient classification of covid-19 CT scans by using q -transform model for feature extraction. *PeerJ Comput. Sci.* **2021**, *7*, e553. [[CrossRef](#)]
4. Ibrahim, Y.; Yahya, R.W.H.; Mohammed, A.J.; Al-Saidi, N.M.G.; Baleanu, D. Mathematical Design Enhancing Medical Images Formulated by a Fractal Flame Operator. *Intell. Autom. Soft Comput.* **2022**, *32*, 937–950. [[CrossRef](#)]
5. Farhan, K.A.; Al-Saidi, N.M.G.; Maolood, A.T.; Nazarimehr, F.; Hussain, I. Entropy analysis and image encryption application based on a new chaotic system crossing a cylinder. *Entropy* **2019**, *21*, 958. [[CrossRef](#)]
6. Nicolas, B. *A Short History of Mathematical Population Dynamics*; Springer: London, UK, 2011.
7. Kermack, W.O.; McKendrick, A.G. A contribution to the mathematical theory of epidemics. *Proc. R. Soc. A* **1927**, *115*, 700–721.
8. Chang, Z.; Meng, X.; Zhang, T. A new way of investigating the asymptotic behaviour of a stochastic sis system with multiplicative noise. *Appl. Math. Lett.* **2019**, *87*, 80–86. [[CrossRef](#)]
9. Huang, W.; Han, M.; Liu, K. Dynamics of an SIS reaction-diffusion epidemic model for disease transmission. *Math. Biosci. Eng.* **2017**, *7*, 51–66.
10. Liu, M.; Chang, Y.; Wang, H.; Li, B. Dynamics of the impact of twitter with time delay on the spread of infectious diseases. *Int. J. Biomath.* **2018**, *11*, 1850067. [[CrossRef](#)]
11. Newman, M.E.J. The structure and function of complex networks. *SIAM Rev.* **2003**, *45*, 167–256. [[CrossRef](#)]
12. Momani, S.; Ibrahim, R.W.; Hadid, S.B. Susceptible-infected-susceptible epidemic discrete dynamic system based on Tsallis entropy. *Entropy* **2020**, *22*, 769. [[CrossRef](#)] [[PubMed](#)]
13. Pastor-Satorras, R.; Vespignani, A. Epidemics and immunization in scale-free networks. In *Handbook of Graphs and Networks*; Wiley: Berlin, Germany, 2003.
14. Colizza, V.; Pastor-Satorras, R.; Vespignani, A. Reaction–diffusion processes and metapopulation models in heterogeneous networks. *Nat. Phys.* **2007**, *3*, 276–282. [[CrossRef](#)]
15. Kang, H.; Sun, M.; Yu, Y.; Fu, X.; Bao, B. Spreading dynamics of an SEIR model with delay on scale-free networks. *IEEE Trans. Netw. Sci. Eng.* **2018**, *7*, 489–496. [[CrossRef](#)]
16. Kuśmierz, Ł.; Toyozumi, T. Infection curves on small-world networks are linear only in the vicinity of the critical point. *Proc. Natl. Acad. Sci. USA* **2021**, *118*, e2024297118. [[CrossRef](#)] [[PubMed](#)]
17. Bae, H.J.; Lee, S. Investigation of SIS epidemics on dynamic network models with temporary link deactivation control schemes. *Math. Biosci. Eng.* **2022**, *19*, 6317–6330. [[CrossRef](#)]
18. Boole, G. *A Treatise on the Calculus of Difference Equations*; Cambridge University Press: Cambridge, UK, 1860; Volume 2, p. 17.
19. Wolfgang, H. Über Orthogonalpolynome, die q -Differenzgleichungen genügen. *Math. Nachrichten* **1949**, *2*, 4–34.
20. Chakrabarti, R.; Jagannathan, R. A (p, q) -oscillator realization of two-parameter quantum algebras. *J. Phys. Math. Gen.* **1991**, *24*, L711. [[CrossRef](#)]
21. Tsallis, C. Possible generalization of Boltzmann-Gibbs statistics. *J. Stat. Phys.* **1988**, *52*, 479–487. [[CrossRef](#)]
22. Ramírez-Reyes, A.; Hernández-Montoya, A.R.; Herrera-Corral, G.; Domínguez-Jiménez, I. Determining the entropic index q of Tsallis entropy in images through redundancy. *Entropy* **2016**, *18*, 299. [[CrossRef](#)]
23. Machado, J.T. Fractional order generalized information. *Entropy* **2014**, *16*, 2350–2361. [[CrossRef](#)]
24. Machado, J.T. Fractional Renyi entropy. *Eur. Phys. J. Plus* **2019**, *134*, 1–10. [[CrossRef](#)]
25. Ibrahim, R.W.; Moghaddasi, Z.; Jalab, H.A.; Noor, R.M. Fractional differential texture descriptors based on the Machado entropy for image splicing detection. *Entropy* **2015**, *17*, 4775–4785. [[CrossRef](#)]
26. Hasan, A.M.; Al-Jawad, M.M.; Jalab, H.A.; Shaiba, H.; Ibrahim, R.W.; AL-Shamasneh, A.A.R. Classification of Covid-19 Coronavirus, Pneumonia and Healthy Lungs in CT Scans Using Q -Deformed Entropy and Deep Learning Features. *Entropy* **2020**, *22*, 517. [[CrossRef](#)] [[PubMed](#)]
27. Ibrahim, R.W. The fractional differential polynomial neural network for approximation of functions. *Entropy* **2013**, *15*, 4188–4198. [[CrossRef](#)]
28. Ibrahim, R.W. Utility function for intelligent access web selection using the normalized fuzzy fractional entropy. *Soft Comput.* **2020**, 1–8. [[CrossRef](#)]
29. Jalab, H.A.; Subramaniam, T.; Ibrahim, R.W.; Kahtan, H.; Noor, N.F.M. New Texture Descriptor Based on Modified Fractional Entropy for Digital Image Splicing Forgery Detection. *Entropy* **2019**, *21*, 371. [[CrossRef](#)]
30. Ibrahim, W.R.; Darus, M. Analytic study of complex fractional Tsallis' entropy with applications in CNNs. *Entropy* **2018**, *20*, 722. [[CrossRef](#)] [[PubMed](#)]
31. Allen, L.J.S.; Van den Driessche, P. The basic reproduction number in some discrete-time epidemic models. *J. Differ. Equ. Appl.* **2008**, *14*, 1127–1147. [[CrossRef](#)]
32. Yong, T. Maximum entropy method for estimating the reproduction number: An investigation for COVID-19 in China. *Phys. Rev. E* **2020**, *102*, 03216.
33. Tsallis, C.; Tirnakli, U. Predicting COVID-19 peaks around the world. *Front. Phys.* **2020**, *8*, 217. [[CrossRef](#)]

34. Pennings, P. COVID19 in numbers- R_0 , the case fatality rate and why we need to flatten the curve. webm Date: 11 March 2020.
35. Heffernan, J.M.; Smith, R.J.; Wahl, L.M. Perspectives on the basic reproduction ratio. *J. R. Soc. Interface* **2005**, *2*, 281–293. [[CrossRef](#)] [[PubMed](#)]
36. Dayi, H.; Huang, Q.; Gao, J. A new entropy optimization model for graduation of data in survival analysis. *Entropy* **2012**, *14*, 1306–1316.
37. Vijay, P.S.; Sivakumar, B.; Cui, H. Tsallis entropy theory for modeling in water engineering: A review. *Entropy* **2017**, *19*, 641.
38. Talu, S. Multifractal geometry in analysis and processing of digital retinal photographs for early diagnosis of human diabetic macular edema. *Curr. Eye Res.* **2013**, *38*, 781–792. [[CrossRef](#)] [[PubMed](#)]
39. Ott, E. *Chaos in Dynamical Systems*; Cambridge University Press: Cambridge, UK; New York, NY, USA, 1993; ISBN 978-0-521-43799-8.
40. Sam, Y.; Lakshminarayanan, V. Fractal Dimension and Retinal Pathology: A Meta-Analysis. *Appl. Sci.* **2021**, *11*, 2376.
41. Huang, F.; Dashtbozorg, B.; Zhang, J.; Bekkers, E.; Abbasi-Sureshjani, S.; Berendschot, T.T.J.M.; Ter Haar Romeny, B.M. Reliability of using retinal vascular fractal dimension as a biomarker in the diabetic retinopathy detection. *J. Ophthalmol.* **2016**, *2016*, 6259047. [[CrossRef](#)]
42. Renyi, A. On the dimension and entropy of probability distributions. *Acta Math. Acad. Sci. Hung.* **1959**, *10*, 193–215. [[CrossRef](#)]
43. Alberti, T.; Donner, R.V.; Vannitsem, S. Multiscale fractal dimension analysis of a reduced order model of coupled ocean-atmosphere dynamics. *Earth Syst. Dyn. Discuss.* **2021**, *12*, 1–24. [[CrossRef](#)]